Meas. Sci. Technol. **18** (2007) 3241–3246 doi:10.1088/0957-0233/18/10/S29

A reconfigurable multimode interference splitter for sensing applications

D A May-Arrioja[1], P LiKamWa[2], J J Sánchez-Mondragón[1], R J Selvas-Aguilar[3] and I Torres-Gomez[4]

[1] Photonics and Optical Physics Laboratory, Optics Department, INAOE, AP 51 y 216, Tonantzintla, Puebla 72000, México
[2] CREOL and FPCE, The College of Optics and Photonics, University of Central Florida, Orlando, FL 32816-2700, USA
[3] Facultad de Ciencias Físico Matemáticas, Universidad Autónoma de Nuevo León, Nuevo León, Monterrey 66450, México
[4] Centro de Investigaciones en Óptica, Lomas del bosque 115, León, Gto. 37150, México

E-mail: dmay@inaoep.mx

Received 31 December 2006, in final form 13 April 2007
Published 12 September 2007
Online at stacks.iop.org/MST/18/3241

Abstract
A reconfigurable multimode interference (MMI) coupler is demonstrated. The device operates by modifying the phase of the multiple images that are formed around the midpoint of the MMI section. This modifies the properties of the following set of images, and light can be directed to a specific output waveguide, which is therefore ideal to develop a reconfigurable MMI coupler. In our device the phase change is achieved by current injection, and therefore minimizing current spreading is crucial for optimal operation. A zinc in-diffusion process has been implemented to selectively define p–n regions and effectively regulate current spreading by controlling the depth of the zinc doping. Using this process, a reconfigurable 3 dB MMI coupler has been fabricated. Our experimental results revealed that the device can be easily set to a perfect 3 dB splitter using only 0.7 mA of current injection. In addition, the device can be adjusted all the way from a 90:10 to a 30:70 splitting ratio. The results are very encouraging since, to our knowledge, this degree of tuning of the optical power has never been experimentally demonstrated in MMI devices. Furthermore, this concept can easily be applied to a wide variety of semiconductor photonic switches that operate on MMI effects.

Keywords: sensors, MMI, multimode interference, tunable coupler, integrated sensor, integrated optics, semiconductor, quantum-well devices

(Some figures in this article are in colour only in the electronic version)

1. Introduction

The development of integrated optical sensors is very attractive because they offer the possibility of integrating different components, which is thus translated into more robust and compact devices. In order to optically detect a change in analyte concentration, we are required to translate this change into a measurable parameter such as intensity or phase. Several material platforms have been used to implement integrated optical sensors. However, the use of III–V semiconductors offers some benefits towards the development of highly integrated devices. Since III–V semiconductors possess a direct band gap, they have the potential for the integration of lasers, waveguides, phase modulator and detectors on a single chip. This is a critical aspect for sensing applications, since this can provide not only compact, but also inexpensive and portable devices. Over the years, a variety of sensing configurations has been implemented. Among them, the Mach–Zehnder interferometer has been widely used because high sensitivity can be achieved without the need for chemical

labelling [1–3]. Nevertheless, their main limitation for size reduction is related to the Y-branches that are typically used for splitting and combining the optical signal. A simple solution is the use of multimode interference (MMI) splitters because they have a compact size, wide optical bandwidth and relaxed fabrication tolerances. They have been widely used in various integrated optical circuits for the splitting or combining of optical signals [4–6]. In order to obtain the largest dynamic range in a Mach–Zehnder-based sensor, it is imperative that the split-off beams must be exactly balanced with a ratio of 50:50. By employing a reconfigurable MMI coupler, an accurate setting of the splitting ratio can readily be accomplished. Furthermore, the reconfigurable MMI coupler can also be used as the beam combiner to compensate for unequal optical intensities in the two arms of the interferometer. Consequently, deviations due to non-uniformity in waveguide propagation losses arising from fabrication errors can readily be tuned out using reconfigurable MMI couplers, thus enabling optimal performance of the interferometric sensor.

In general, reconfigurable MMI couplers can be obtained in two ways. The first one requires modifying the phase relation between the even and odd modes that are propagating along the MMI waveguide [4]. Since the phase is modified on a narrow section along the whole MMI, a smaller refractive index change is then required. However, it is difficult to modify the phase of the even modes only without a slight change of the phase of the odd modes. A better approach is to modify the phase of the multiple self-images that occur at different lengths along the MMI waveguide. Modifying the phase relation between the self-images leads to a modified output image, and light can be directed to a specific output waveguide [7, 8]. If the refractive index change is entirely confined within the areas containing the principal self-images, very efficient devices could be realized using this approach. However, due to the refractive index change requirements they are intended to operate by current injection (carrier-induced refractive index change). In this case, current spreading becomes a serious issue in terms of device performance. It is therefore necessary to electrically isolate the index-modulated regions in order to regulate the current spreading within the MMI waveguide.

In this work, current spreading is controlled by using a zinc in-diffusion technique to achieve a selective definition of p–n regions [9]. The zinc in-diffusion process is performed using a semi-sealed open-tube diffusion furnace. The method has proven to be simple, yet highly controllable and reproducible. Using this technique, current spreading is effectively regulated, making it ideal for fabricating electrically tunable optical MMI couplers. This process was used to fabricate a reconfigurable 3 dB MMI coupler that was modified all the way from a nearly 50:50 split of output powers to a 90:10 splitting ratio by injecting current through edge contacts, and to a 30:70 splitting ratio when a centre electrode was used.

2. Multimode interference couplers

The analysis of MMI devices has been approached using different methods such as ray optics [10], beam propagation method (BPM) [11] and guided-mode propagation analysis (MPA) [4]. Among these methods, the MPA provides better insight into the mechanism behind the MMI functionality. The operation of a MMI device is relatively simple. The key component is a multimode waveguide that supports several modes ($\geqslant$3). After the supported modes are excited by launching a field using an input waveguide (typically, a single mode waveguide), the interference between the modes propagating along the MMI waveguide gives rise to the formation of self-images (single and multiple) of the input field, as shown in figure 1. For simplicity, only the formation of single and two-fold self-images is shown.

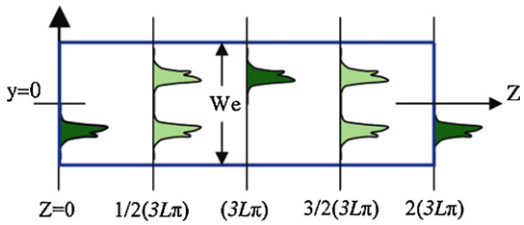

Figure 1. Self-image formation along a multimode waveguide showing single and two-fold images.

In the case of general interference, the formation of the self-images (single and multiple) along the multimode waveguide is given by

$$L = \frac{p}{N}(3L_\pi), \tag{1}$$

where $p \geqslant 0$ and $N \geqslant 1$ are integers with no common divisor [4]. Here N is related to the number of self-images and p denotes the periodic nature of the imaging along the multimode waveguide for each set of N images. In this case, L_π is defined as the beat length between the two lowest order modes

$$L_\pi = \frac{\pi}{\beta_0 - \beta_1} \cong \frac{4n_0 W_e^2}{3\lambda_0}, \tag{2}$$

where W_e is the effective multimode waveguide width, n_0 is the effective refractive index and λ_0 is the vacuum wavelength. In order for these equations to hold at any position, it is necessary to maintain certain conditions related to the modes and self-images.

(1) The first condition requires that all the modes should experience a 2π phase shift after propagating along the multimode waveguide up to the position of the first self-image, thus producing a direct replica of the input field.
(2) In addition, the phase differences between the propagating modes must alternate in even and odd multiples of π, with the even and odd modes in phase and antiphase respectively. Therefore, the single self-images will be mirrored with respect to $y = 0$ as compared to the previous single self-image. This is, of course, not a concern for symmetric input fields as in the case of single-mode input waveguides.
(3) Regarding the multiple self-images, there is a well-established relative phase difference between the images on each set of images. Therefore, this phase relationship needs to be kept constant for proper formation of the following set of images at distances dictated by the previous equations.

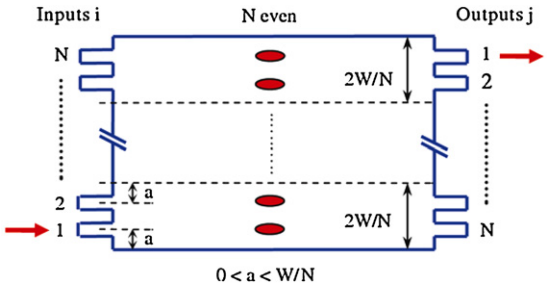

Figure 2. MMI coupler illustrating $N \times N$ operation for the case of N even inputs.

As long as these conditions are met, the operation of the designed MMI device should be very stable without any variation of the designed output or splitting ratio, in the case of MMI splitters. MMI devices designed under the condition of general interference are very compact devices with large optical bandwidths and relaxed fabrication tolerances. However, in integrated devices there is always a need for smaller devices in order to maximize the wafer real state. In the case of MMI devices, if we can selectively excite certain modes within the MMI waveguide, the MMI length can be further reduced. This can be achieved by launching a symmetric input field at $y = \pm W_e/6$; at this position the modes $\nu = 2, 5, 8, \ldots$ present a zero with odd symmetry with respect to this point. Therefore, the overlap integral between the input field and these modes will vanish. As a result, only the first two of every three modes are excited, and the length of the self-images is reduced by one third [4]. Under this restricted paired interference mechanism, the position of the self-images can still be found using (1), but we have to reduce it by one third.

3. Active MMI couplers

The majority of the applications of MMI devices up to date have been related to passive devices. Only recently has there been a major effort to obtain active devices because of the size reduction and performance that can be achieved. In general, active MMI devices can be obtained by perturbing the conditions required for self-images to occur at the predicted locations, such as changing the phase relation between the multiple images and selective mode perturbation. Selective mode perturbation requires modifying the phase of the even modes without perturbing the phase of the odd modes [12]. In practice, this is not a simple task to achieve since all the modes are propagating along the same waveguide. A better approach is to modify the phase relation between the multiple images at some specific locations. As previously explained, the phase relation of each set of multiples images has to stay constant for the next set to be properly formed. If we selectively modify the phases in a particular set, then the phases and lateral positions of the following sets of images will be modified. With the right parameters this effect can be used to develop not only reconfigurable MMI couplers, but also photonic switches [7, 8]. The principle can be better explained by looking at the general picture of an $N \times N$ MMI coupler, as shown in figure 2.

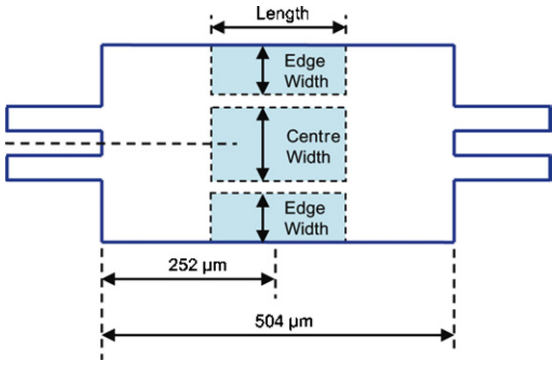

Figure 3. Schematic of the reconfigurable MMI coupler and design parameters.

In this $N \times N$ MMI coupler, light directed into any of the N inputs is equally split into N images right at the middle point of the MMI coupler, but the relative phases of these N images will be different for each input waveguide. The expressions for calculating the phases of the N images for the case of N even inputs are given by [13]

$$i + j \text{ even}, \quad \varphi_{ij} = \pi + \frac{\pi}{4N}(j - i)(2N - j + i) \tag{3}$$

$$i + j \text{ odd}, \quad \varphi_{ij} = \frac{\pi}{4N}(j + i - 1)(2N - j - i + 1). \tag{4}$$

Knowing the phase value of each of the N images for each input, light coupled to any given input can be switched to any output by properly modifying these N phases. For example, in this particular $N \times N$ coupler, light directed to the input will exit at the output, with the N images having a specific phase relation. If this phase relation is modified such that it replicates the phase relation obtained when light is directed to input N, then the light can be switched to output N. A similar principle can be applied by modifying the phase at a different set of images, and this will modify the properties of the following sets. This concept is used in this work to achieve a reconfigurable MMI splitter.

In order for such devices to operate properly, the refractive index change has to be entirely confined within specific areas containing the principal self-images. If this can be achieved, very efficient devices could be realized using this approach. However, due to the refractive index change requirements they are intended to operate by current injection (carrier-induced refractive index change). In this case, current spreading becomes a serious issue in terms of device performance and makes it necessary to electrically isolate the index-modulated regions in order to regulate the current spreading within the MMI waveguide. We have previously demonstrated that current spreading can be efficiently controlled using a selective zinc in-diffusion technique to achieve a selective definition of p–n regions [9]. A similar process will be used in order to confine the refractive index change within the required image.

4. MMI splitter design

A schematic of the reconfigurable MMI coupler is shown in figure 3. It consists of a multimode waveguide section that has

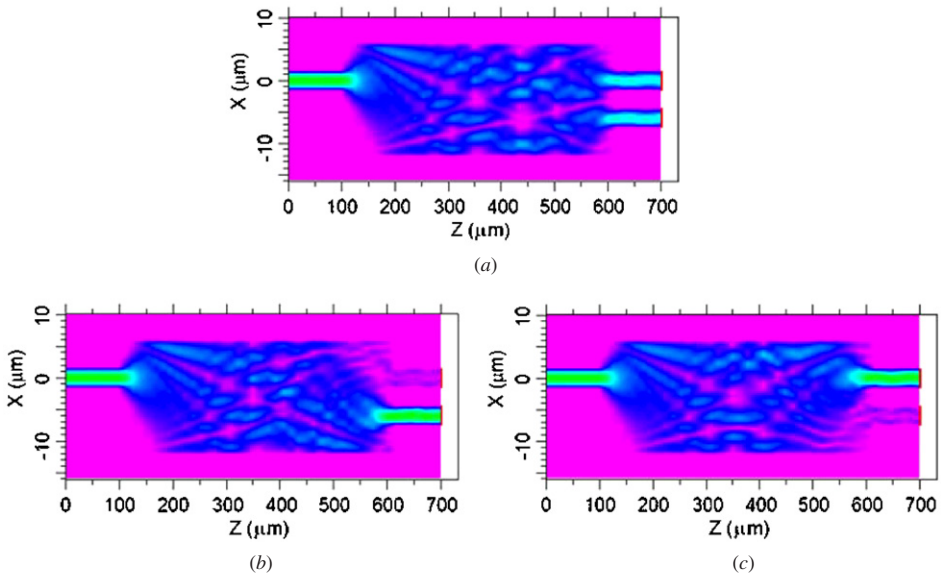

Figure 4. Beam propagation characteristics of reconfigurable MMI coupler for (*a*) no applied bias, (*b*) centre biased electrode and (*c*) edge biased electrodes.

a width of $W = 18$ μm and a length of $L = 504$ μm. The light is directed into the device using 3 μm wide input and output waveguides that are separated by 3 μm. The shaded areas at the centre of the MMI correspond to the index-modulated regions. The location of these zones corresponds to the areas where the multiple self-images are formed. The dimensions of the MMI coupler have been calculated using the well-known relations for restricted paired interference in MMI waveguides that we previously explained. The wafer structure used for the calculations consists of an undoped InGaAsP MQW core waveguide with a total thickness of 0.28 μm. This layer is bounded on the top and bottom by n-doped InP cladding layers to form a symmetric slab waveguide structure. The top cladding layer is 1.7 μm thick while the lower cladding layer is 1.0 μm thick. The whole structure is capped by a 0.1 μm thick InGaAs layer.

The beam propagation characteristics of the device have been investigated using the finite difference beam propagation method (FD-BPM), which is the core of the commercial software BeamPROP from RSoft. As shown in figure 4(*a*), when light is launched into either input waveguide without any external bias, the device operates as a perfect 3-dB coupler. The formation of multiple images can also be observed at different intervals along the MMI. In this case, we will focus our attention on the four images that are formed exactly at the halfway point along the MMI length. As explained, a well established relative phase exists between these images which control the formation of the subsequent self-images. Therefore, by modifying the phases of these images, the splitting ratio of the MMI coupler can easily be altered. Using (3) and (4), we found that if the phase of the two inner images is altered by $\pi/2$, then all the light is switched to the lower output waveguide. A similar phase change is required for the two edge images for the light to be switched to the upper output waveguide. In order to find the physical dimensions of the areas where the index change will be applied, it was assumed that the current injection resulted in a refractive index change of $(\Delta n/n) = 0.5\%$. Using this value, the dimensions of the index modulated regions were calculated such that the light could be switched from one output port to the other. As shown in figure 3, a central electrode with a length of 65 μm and a width of 8 μm was calculated to provide sufficient phase modification of the two inner images. When this central contact is biased, the light is fully switched to the lower output waveguide as shown in figure 4(*b*). In a similar way, edge electrodes with the same length and a 4 μm width are needed to switch the light into the upper waveguide. This is also shown in figure 4(*c*).

5. Reconfigurable MMI splitter fabrication

The device was fabricated by first covering the whole wafer with a 200 nm thick silicon nitride (Si_3N_4) film. This film acts as a diffusion barrier for the zinc in-diffusion process. Photolithography was then used to pattern windows on the index-modulated areas, and the unwanted Si_3N_4 film was etched off using reactive ion etching (RIE). The zinc in-diffusion process was then performed as explained in [9]. A diffusion time of 30 min resulted in a diffusion depth of 0.8 μm with a sharp diffusion profile. The diffusion process is highly reproducible giving rise to repeatable diffusion depth and doping concentration provided that the diffusion temperature and time are carefully controlled.

After the diffusion, Ti/Zn/Au p-type contacts were patterned on the zinc-diffused areas by photolithography followed by evaporation and lift-off. The MMI structure was then patterned by photolithography, followed by selective wet chemical etching of the InGaAs top layer using a H_3PO_4:H_2O_2:DI water (1:1:38) mixture. The InGaAs layer was then used as a mask for the selective wet etching of InP using an HCl:acetic acid (1:6) mixture. An etch-stop layer provided precise control of the etch depth, resulting in constant

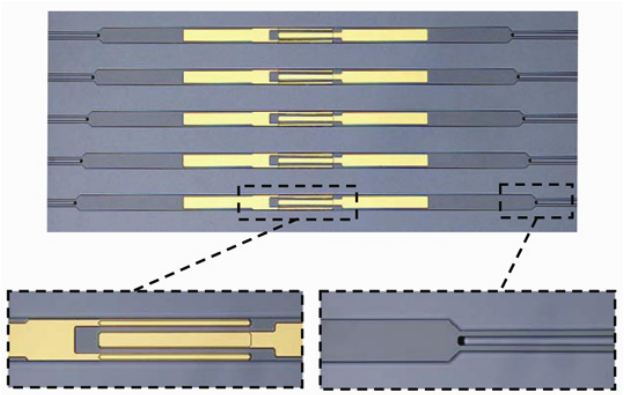

Figure 5. Pictures of the fabricated reconfigurable MMI coupler.

height InP ridges as well as a smoothly etched surface. The wafer substrate was then lapped to a thickness of 150 μm and polished to a mirror finish. The n-type contact, consisting of a mixture of Ni/Ge/Au, was then deposited by thermal evaporation and annealed-in. At this point, the sample was cleaved, and mounted on a copper holder for device testing. A photograph of the top view of a fabricated batch of devices is shown in figure 5. Each batch consists of five MMIs of slightly different lengths in order to compensate for any fabrication error and obtain the closest 3 dB splitter. The MMI at the centre corresponds to the optimum MMI dimensions as calculated from our FD-BPM simulations. The angled corners at the end sections are a result of the different etching planes inherent to InP in acidic etchants.

6. Experimental results

The fabricated devices were tested using a fibre pigtailed tunable laser set at a wavelength of 1560 nm. This wavelength was selected so as to obtain the best 3 dB splitting. The laser beam was then collimated using a fibre collimator and end-fire coupled to the single-mode input waveguide of the device using a 40× microscope objective. The near-field pattern of the output facet was then imaged onto a CCD camera using a 40× microscope objective, and a TV monitor was used to observe the output facet. Two separate laser diode drivers were used to inject electrical current through either the inner contact or the edge contacts.

The normalized output intensity versus applied current characteristics of the device is shown in figure 6(*a*). It can be seen that with no current applied, the splitting ratio is not exactly 50:50 even when five different MMI lengths were fabricated. However, this can be easily adjusted by injecting current into the patterned electrodes. When the edge electrodes are biased, the splitting ratio can be easily switched to better than a 90:10 splitting ratio. We should also note that during the first 3 mA of current injection, the splitting ratio is only slightly modified. We believe that this is caused by a modification of the imaging due to strain from the Si_3N_4 and p-type contacts, which are located on top of the multimode waveguide. However, as evidenced in figure 6(*a*), the injection of only a small current (0.7 mA) through the centre electrode is required to trim the device for an exact 50:50 split of the output powers. By increasing the applied current, the splitting ratio can be changed to a 30:70 split ratio in the other direction. After this point, the behaviour deviates significantly from the theoretically expected response. We believe that at this point, the injected electrons have spread too far beyond the optimum index-modulated region and therefore the device stops working properly. Also shown in figure 6(*b*) are pictures of the output facet for the cases of no bias applied and for the maximum splitting ratios with electrical current injected into the edge and centre contacts respectively.

From these results, it is clear that the coupler can be easily set to a perfect 3 dB splitter which compensates for any fabrication errors. We should also note the fact that such a modification is achieved using a small amount of electrical current injection. Even more important is the fact that, to our knowledge, such an amount of tuning of the optical power has never been experimentally achieved in MMI couplers. This is a very promising technique, since a similar concept can be used to fabricate integrated photonic switches using MMI devices.

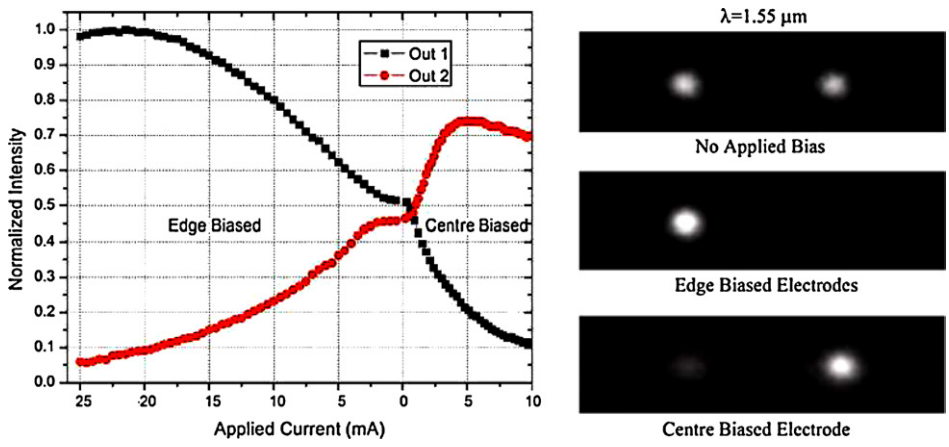

(*a*) (*b*)

Figure 6. (*a*) Response of the reconfigurable MMI coupler as a function of electrical current injection and (*b*) pictures of the device output facet for different biases.

The main limitation to achieving full switching in our current device is that we were interested in trimming the coupler to a 3 dB splitter. Therefore, because the metal electrodes/bonding pads lie directly on top of the MMI region, they add a strain-induced uniform index change that is shifting the position of the multiple images. The effect is that the images do not perfectly overlap with the electrical injection regions, and more current is required for the tuning of the output power split ratio which eventually deteriorates the device performance. As demonstrated, this is not a serious issue for our current 3 dB trimming application. However, it is very critical for devices requiring full switching of the optical signal. This can be easily solved by planarizing the waveguide structure and fabricating the metal pads outside the MMI region.

7. Conclusions

A reconfigurable MMI coupler has been fabricated using a simple zinc in-diffusion process. This technique allows for the selective definition of p–n regions and effectively regulates the current spreading. Our experimental results revealed that the device can be easily set to a perfect 3 dB splitter using only 0.7 mA of current injection. In addition, the device can be adjusted all the way from a 90:10 to a 30:70 splitting ratio. We believe that with further improvements to the device design, full-range switching could also be obtained. The results are very encouraging since, to our knowledge, this amount of tuning of the output power splitting has never been experimentally demonstrated before. Furthermore, since this mechanism can be implemented in several material platforms, the process can be extended to a variety of highly functional integrated photonic devices that operate on MMI effects. This includes sensors, modulators (electro-optic and all-optical) and switches, thus providing a high number of potential applications.

References

[1] Hsu S H and Huang Y T 2005 A novel Mach–Zehnder interferometer based on dual-ARROW structures for sensing applications *J. Lightwave Technol.* **23** 4200–6

[2] Maisenhölder B, Zappe H, Kunz R E, Riel P, Moser M and Edlinger J 1997 A GaAs/AlGaAs-based refractometer platform for integrated optical sensing applications *Sensors Actuators* B **39** 324–9

[3] Maisenhölder B, Zappe H, Moser M, Riel P, Kunz R E and Edlinger 1997 Monolithically integrated optical interferometer for refractometry *Electron. Lett.* **33** 986–8

[4] Soldano L B and Pennings E C M 1995 Optical multi-mode interference devices based on self-imaging: principles and applications *J. Lightwave Technol.* **13** 615–27

[5] Levy D S, Park K H, Scarmozzino R, Osgood R M, Dries C, Studenkov P and Forrest S 1999 Fabrication of ultracompact 3-dB 2 × 2 MMI power splitters *IEEE Photon. Technol. Lett.* **11** 1009–11

[6] Spiekman L, Oei Y, Metaal E, Groen F, Moerman I and Smit M 1994 Extremely small multimode interference couplers and ultrashort bends on InP by deep etching *IEEE Photon. Technol. Lett.* **6** 1008–10

[7] Lien C H, Lin H H, Weng S W, Wang H J and Chang W C 2002 A compact photonic switch based on multimode interference with partial index-modulation regions *Microw. Opt. Technol. Lett.* **33** 174–6

[8] Yagi M, Nagai S, Inayoshi H and Utaka K 2000 Versatile multimode interference photonic switches with partial index-modulation regions *Electron. Lett.* **36** 533–4

[9] May-Arrioja D A, Bickel N and LiKamWa P 2005 Optical beam steering using InGaAsP multiple quantum wells *IEEE Photon. Technol. Lett.* **17** 333–5

[10] Ulrich R and Ankele G 1975 Self-Imaging in homogeneous planar optical-waveguides *Appl. Phys. Lett.* **27** 337–9

[11] Liu G J, Liang B M, Li Q and Jin G L 2005 Beam propagation in nonlinear multimode interference waveguide *J. Opt. A: Pure Appl. Opt.* A **7** 457–62

[12] Earnshaw M P and Allsopp D W E 2002 Semiconductor space switches based on multimode interference couplers *J. Lightwave Technol.* **20** 643–50

[13] Bachmann M, Besse P A and Melchior H 1994 General self-imaging properties in $N \times N$ multimode interference couples including phase-relations *Appl. Opt.* **33** 3905–11